

⁶⁰Co γ -irradiation Effects on Electrical Characteristics of Monocrystalline Silicon Solar Cell

Khuram Ali*, Sohail A. Khan, M.Z. MatJafri

Nano-Optoelectronics Research and Technology Laboratory, School of Physics, Universiti Sains Malaysia, Penang 11800, Malaysia

*E-mail: khuram_uaf@yahoo.com

Received: 1 March 2013 / Accepted: 27 April 2013 / Published: 1 June 2013

We report the gamma-ray (γ -ray) radiation-induced defects incurred by a monocrystalline Si solar cell. Capacitance–voltage (C – V) and dark current–voltage (I – V) characteristics were investigated from 1 kHz to 100 kHz at room temperature. The Co^{60} activity used for the γ -ray irradiation of a Si solar cell was 24864.37 atom Bq. The laboratory-made solar cell was irradiated at a 2π solid angle for 60 and 150 min. Results revealed that all output parameters, namely, short-circuit current, open-circuit voltage, fill factor, and relative efficiency, were degraded after irradiation. The dark I – V and non-ideality factor increased with increasing irradiation. C – V frequency measurements revealed the presence of the Compton scattering effect and radiation-induced defects. These defects were heavily occupied by electrons. Irradiation increased the density of defects and reduced the barrier height and overall cell efficiency.

Keywords: degradation; gamma irradiation; capacitance; solar cell

1. INTRODUCTION

Solar cells are widely used in satellites as auxiliary power sources. The importance of these cells in space research cannot be repudiated. Solar cells are extremely sensitive to electromagnetic radiation with substantially short wavelengths, such as x-rays and gamma-rays (γ -rays) [1–4]. These types of radiation are abundantly available in space and are widely used to study ionization-induced damage in devices [5]. These types of high-energy radiation cause lattice defects in semiconductor devices; such defects decrease the output power of solar cells [6, 7]. Any changes caused by γ -rays, neutrons, or charged particles in the lattice periodicity result in additional energy levels in the band gap. These new energy levels alter the electrical properties of solar cells because of the electron-hole pairs generated near the mid gap [8–10]. Energy centers increase the leakage current. Other factors

attributed to γ -ray irradiation are also involved in the characteristic changes of solar cells. Such factors include the recombination of electron-hole pairs, trapping of electron-hole pairs, compensation of free electrons or holes by radiation-induced centers, and tunneling of carriers (Figure 1) [11].

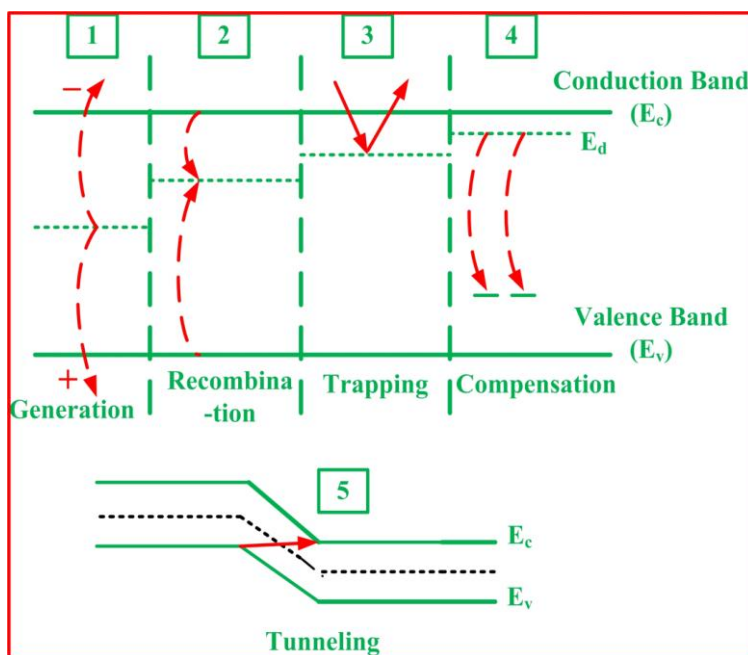


Figure 1. Different Effects due to defect centers in the silicon bandgap.

These factors are important in characteristic changes; however, these factor are dependent on certain variables [12, 13] such as temperature, electron or hole concentration in the semiconductor, and electron or hole region (e.g., depletion region) [14].

1.1 Compton Scattering

Electrons and secondary photons are produced when γ -rays pass through matter. This phenomenon is called the Compton scattering effect, which produces considerable electrons. The photoelectric effect and pair production are negligible in the photon energy range. A photon that interacts with a Si solar cell removes the primary electron from an atom. Each primary electron removed from ionizing collisions produces a swift secondary electron that may contain nearly as much kinetic energy as the primary photon. The secondary electron dissipates its energy as kinetic energy, thereby ionizing and exciting the atoms in the absorber [11]. This kinetic energy is eventually dissipated in the medium as heat and imparted to the atom; the kinetic energy then displaces the atom from its normal site, thus producing a vacancy-interstitial pair [15]. Defects in regions containing high electric fields enhance the effectiveness of the thermal generation of carriers by reducing the potential barrier; this phenomenon is called the Poole–Frenkel effect [14]. The minimum energy E_d in Si is

approximately 13 eV [16]. The energy E_t needed by an electron to impart E_d to the struck atom is related to E_d based on the following relationship [17].

$$E_d = \frac{2m_e}{M_2} \frac{E_t}{m_e c^2} (E_t + 2m_e c^2) \quad (1)$$

For silicon, E_t is about 0.14 meV. Seitz and Koehler [17] present a displacement cross section for electrons, $\sigma_{d1}(E)$;

$$\sigma_{d1}(E) = \frac{\pi b'^2}{4} \left[\left(\frac{T_m}{E_d} - 1 \right) - \beta^2 \ln \left(\frac{T_m}{E_d} \right) + \pi \alpha \beta \left\{ 2 \left[\left(\frac{T_m}{E_d} \right)^{\frac{1}{2}} - 1 \right] - \ln \frac{T_m}{E_d} \right\} \right] \quad (2)$$

$$\text{Where } \frac{\pi b'^2}{4} = \pi z_2^2 \left(\frac{e^2}{m_e c^2} \right)^2 \frac{1}{\beta^4 \gamma^2}$$

In order to complete the calculation of the number of atoms displaced by a gamma flux, we also need the energy distribution $n(E)$ of the Compton electrons. This relation is readily available from the literature [18]. Thus, the number of atoms N_γ displaced from their normal lattice sites by a gamma ray can be calculated by the following relation.

$$N_\gamma = n_o X \int_{E_t}^{E_m} n(E) \sigma_{d1}(E) dE \quad (3)$$

Where E_t is the minimum electron energy needed to displace an atom and E_m is the maximum energy the Compton electron can have, n_o is the molecular density and X the thickness of the material.

With this as an incentive, electrical measurements [19, 20] have been made to predict the performance of silicon solar cell, irradiated with gamma rays. In this experiment mono-crystalline silicon solar cell has been irradiated with Co^{60} gamma rays, and the results presented using C-V and I-V characteristics.

2. EXPERIMENTAL

Boron-doped p-type (100) oriented Si wafers at 10 mm × 10 mm were used. The wafers were cleaned by the RCA standard clean method followed by a 20 s dip in a 10:1 H₂O:HF solution. After rinsing by de-ionized water and blowing by N₂, the wafers were baked for 10 min at 100 °C to remove moisture. The p-n junction was created in a quartz tube furnace at 1000 °C. Contacts on both sides of the sample were thermally evaporated from a tungsten filament at 3 × 10⁻⁵ torr in an oil vacuum pump system. The back side contact was created on the entire back surface with high purity Al (99.999%), whereas the front side contact was made with Ag (350 nm) followed by Al (200 nm) by using a metal grid mask. Thereafter, the wafers were sintered at 400 °C for 15 min under flowing N₂ (3 L·min⁻¹) to form good ohmic contacts. The grid structure of solar cells consists of metal mask grid pattern with finger spacing of 0.65mm, and finger width of 0.30mm. After fabrication the device was characterized before and after Co^{60} γ -ray irradiation (1 μCi). Capacitance voltage (C-V) and dark I-V characteristics were carried out by using semiconductor parameter analyzer (Model 4210-CVU, Keithley). The photocurrent measurements were obtained using a simulator (Leios IV SolarCT) under air mass 1.5

(100 mW/cm²) and white light illumination conditions. The Co⁶⁰ radiant flux was 24864.37 atom Bq at the time of the experiment calculated from the half-life. The following equation was used to calculate the rate constant *k*,

$$\ln N - \ln N_o = -k \left(t^{1/2} \right) \tag{4}$$

where *N* is the amount of radioisotope at the moment the rate is measured, and *N_o* is the initial amount of the radioisotope. The sample was irradiated with Co⁶⁰ γ-rays emitting at a 2π solid angle by following the method used to measure the amount of radiant flux from the gamma source.

$$\Delta I = A \left(\frac{d\Omega}{4\pi} \right) \tag{2.2} \quad \text{where} \quad d\Omega = \frac{a}{r^2}$$

Where *r* is the distance between source and sample while “*a*” is the area on which radiant flux $\Omega = 2\pi(1 - \cos \Phi) = 4\pi \sin^2 \frac{\Phi}{2}$ (5)

The ideality factor *η* can be determined from the slope of the I-V curve. Following equation has been used to determine the ideality factor from the slopes of the Fig. 2 [21, 22].

$$\eta = q/kT \left(V_2 - V_1 / \ln(I_2/I_1) \right) \tag{6}$$

Where, *kT/q* is the thermal voltage at 300 K (0.026 V)

3. RESULTS AND DISCUSSION

3.1 Current Voltage (I-V) measurements

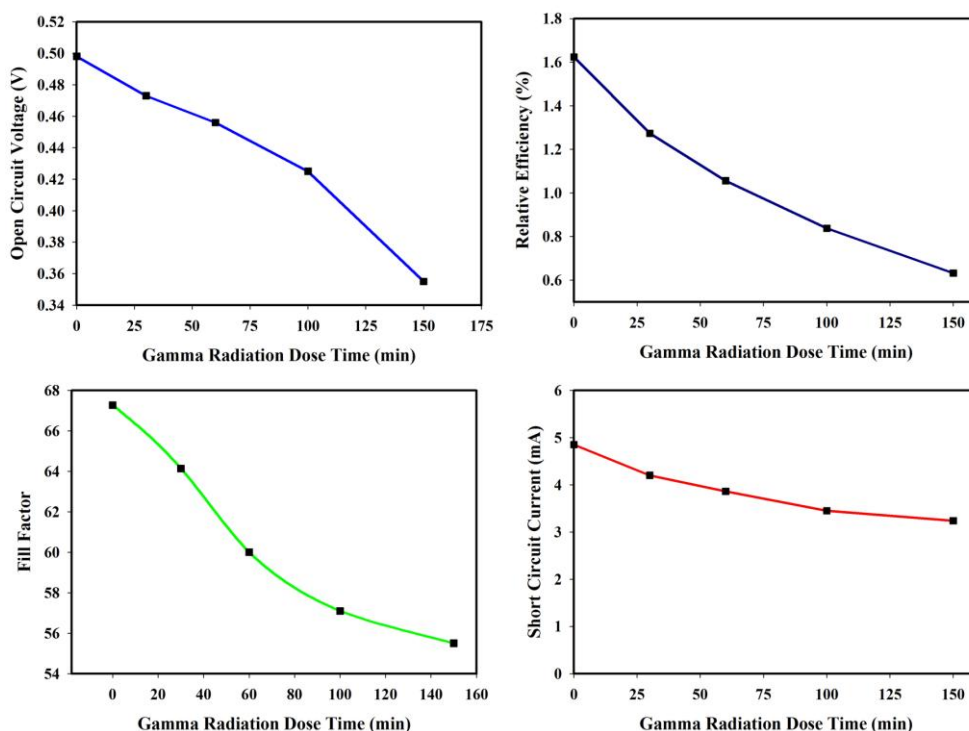


Figure 2. Effect of irradiation time on different output characteristics of monocrystalline silicon solar cell, (a) open circuit voltage, (b) short circuit current, (c) fill factor, (d) relative efficiency.

Figure 2 shows the output parameters of the monocrystalline Si solar cell obtained from the measured current–voltage (I – V) curves. All output parameters, namely, open-circuit voltage V_{oc} , short-circuit current I_{sc} , fill factor, and conversion efficiency of the monocrystalline Si solar cell, were degraded. These changes in the electrical properties of the solar cell were attributed to the additional energy levels in the band gap. These additional energy levels were caused by the dissipation of kinetic energy in the medium as heat energy. This behavior was consistent with the following equation.

$$I \propto e^{(-E_g/2k_B T)} \tag{7}$$

The dark I – V characteristics of the monocrystalline Si solar cell were further analyzed to study the degradation mechanism of γ -ray irradiation. For example, Figure 3 shows the γ -ray irradiation degradation effect on the dark semi-logarithmic I – V characteristics before and after irradiation for 60 and 150 min; the value of the non-ideality factor increased from 2.56 to 3.51. This increase was caused by the increasing density of energy states, which act as generation–recombination centers, thereby increasing the dark current by creating new paths and reducing photocurrent [23].

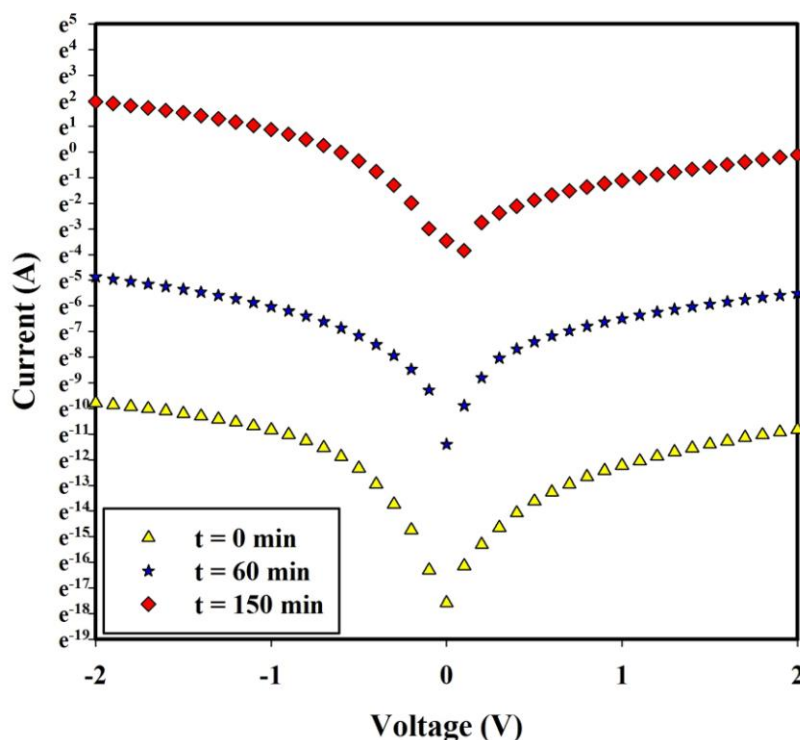


Figure 3. Effect of irradiation time on dark I-V characteristics of monocrystalline silicon solar cell.

The dark characteristics can be described by the expression:

$$J = J_s \left[\exp\left(\frac{eV}{nkT}\right) - 1 \right] \tag{8}$$

where J_s represents the saturation current density, and n denotes the diode non-ideality factor. J_s and n depend on the carrier transport mechanism [24–27]. The different mechanisms involved in the thermal generation of carriers caused by photon–matter interactions can be described as follows.

3.2 Compton Interactions

Photon–matter interactions were dependent only on the quantum energy, $E' = h\nu$, and exhibited an exponential attenuation. Due to law of conservation of momentum and scattering angle, the quantum energy and momentum of scattered photon must be less than that of incident photon. The remaining momentum and energy were imparted to the struck electron; the resulting energy can be described as absorbance. The average energy absorbed per unit volume in an absorber as a result of Compton interactions is simply $I_o\sigma_a$ ergs/ (cm³·s) [28]. In absolute values, ${}_e\sigma_s$ and σ_s any absorber that passed through a maximum when $\alpha = 1$, that is, when $h\nu_o = 0.51$ MeV.

3.2.1 Compton Scattering Coefficients ${}_e\sigma_s$ and σ_s

The total energy ${}_eQ$ scattered in a time t by one electron, from a beam having incident intensity I_o , is

$$\frac{{}_eQ}{t} = \frac{1}{t} \int d({}_eQ) = I_o \int_0^\pi d({}_e\sigma_s) \equiv I_o ({}_e\sigma_s) \tag{9}$$

Where average scattering cross section ${}_e\sigma_s$ is

$${}_e\sigma_s = \pi r_0^2 \left[\frac{1}{\alpha^3} \ln(1+2\alpha) + \frac{2(1+\alpha)(2\alpha^2 - 2\alpha - 1)}{\alpha^2(1+2\alpha)^2} + \frac{8\alpha^2}{3(1+2\alpha)^3} \right] \text{ cm}^2/\text{electron} \tag{10}$$

Or, for sufficiently small values of incident energy α [29]

$${}_e\sigma_s = \frac{8\pi}{3} r_0^2 (1 - 3\alpha + 9.4\alpha^2 - 28.0\alpha^3 + \dots) \text{ cm}^2/\text{electron} \tag{11}$$

Note that ${}_e\sigma_s$ approaches the Thomson cross section of $\frac{8\pi}{3} r_0^2 = \frac{2}{3}$ barn as the photon energy decreases. This is because in the Thomson case all energy is scattered and none is absorbed by the electron while the average energy per scattered photon $(h\nu')_{av}$, or the average scattered energy per collision, is

$$h\nu' = h\nu_o \frac{{}_e\sigma_s}{\sigma} \tag{12}$$

Each scattered photon $h\nu'$ has associated with it a recoil electron whose energy is

$$T = h\nu_o - h\nu' \tag{13}$$

The average scattered energy given by ${}_e\sigma_s$, Eq. (#), while the total energy ${}_e\sigma$ removed from the incident beam by Compton collisions is given by following Eq.

$${}_e\sigma = 2\pi r_0^2 \left\{ \frac{1+\alpha}{\alpha} \left[\frac{2(1+\alpha)}{1+\alpha} - \frac{1}{\alpha} \ln(1+2\alpha) \right] + \frac{1}{2\alpha} \ln(1+2\alpha) - \frac{1+3\alpha}{(1+2\alpha)^2} \right\} \text{ cm}^2/\text{electron} \tag{14}$$

It is now obvious, from conservation of energy, that the energy absorbed by the electron must be the total energy involved in collisions minus the energy scattered as photons, and so we can write for the average absorption cross section, ${}_e\sigma_a$,

$${}_e\sigma_a = \sigma_a - {}_e\sigma_s \tag{15}$$

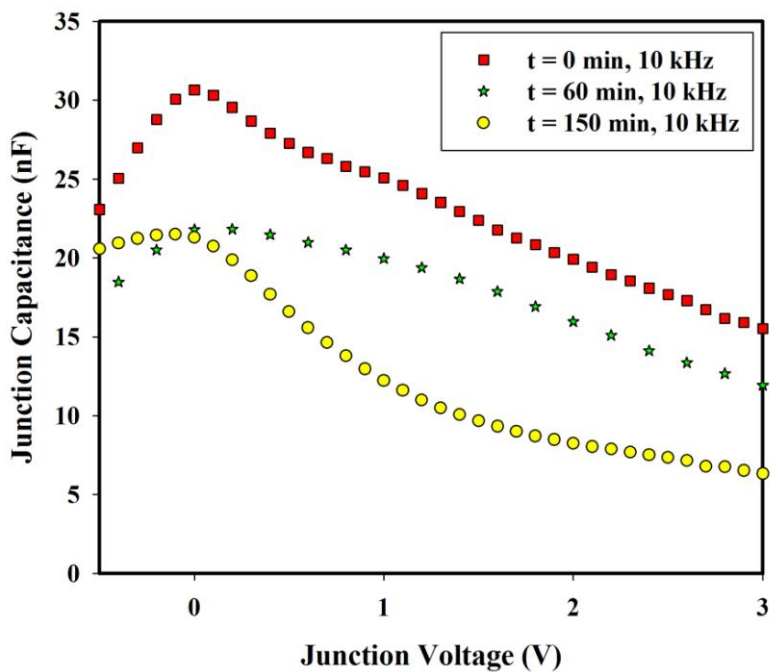


Figure 4. Capacitance-voltage characteristics of monocrystalline solar cell at 10 kHz.

3.2.2 Average Energy per Compton Electron

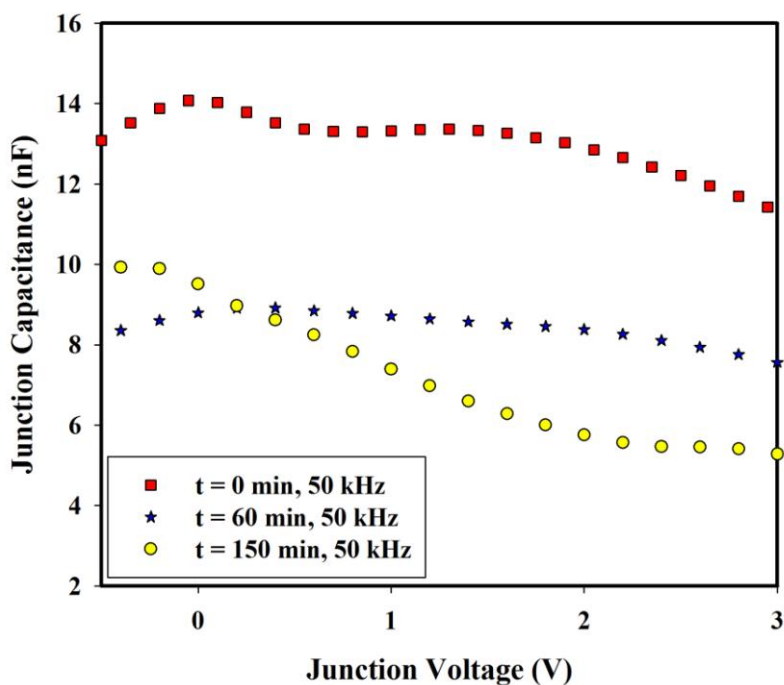


Figure 5. Capacitance-voltage characteristics of monocrystalline Si cell at 50 kHz

The average kinetic energy $(T)_{av}$ of all recoil electrons from Compton interactions will be

$$(T)_{av} = hv_0 - (hv')_{av} \tag{16}$$

$$\text{Hence } \frac{(T)_{av}}{h\nu_0} = 1 - \frac{(h\nu')_{av}}{h\nu_0} = 1 - \frac{e\sigma_s}{e\sigma} = \frac{e\sigma_a}{e\sigma} \tag{17}$$

Thus we see that $e\sigma_a$ physically represents a true absorption of energy from the incident photon and not just a deflection. This absorbed energy appears in the absorbing body as the kinetic energy of the recoil or Compton electrons. These electrons then lose their energy in ionizing and radiative collisions [25]. $e\sigma$, representing the probability of any kind of collision, $e\sigma_s$, representing scattering, or mere deflection of electromagnetic radiation and $e\sigma_a$, representing true absorption of energy from the electromagnetic radiation.

3.3 Frequency dependency of capacitance-voltage (C–V) measurements

Cell capacitance (C) shifted toward a lower value with increasing frequency (Figures 4, 5 and 6); these figures also depict the existence of recombination centers or energy states. This increase in energy states was attributed to the increase in low-frequency C with increasing irradiation time. Barrier height could be determined from the $1/C^2$ –V curves [30] measured at 10 kHz for different γ -ray irradiation times (Figure 7). Plotting the intercept of the straight line of the C with the x-axis allowed V_{bi} to be deduced according to Eq. (6).

$$\frac{1}{C^2} = \left(\frac{1}{q\epsilon_s N_a} \right) (V - V_{bi}) \tag{18}$$

where ϵ_s semiconductor permittivity and N_a concentration of acceptor atoms.

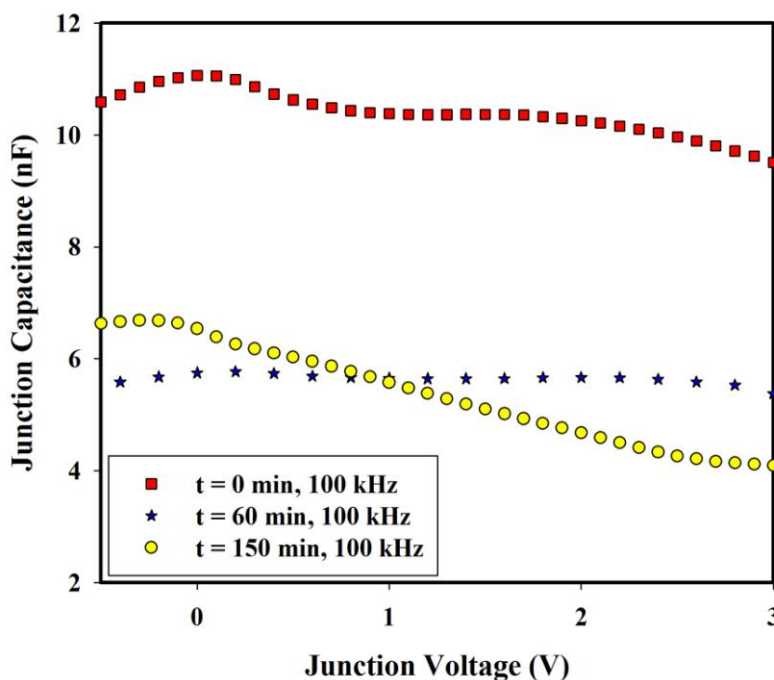


Figure 6. Capacitance-voltage characteristics of monocrystalline Si cell at 100 kHz

Energy states produced from γ -ray irradiation were heavily occupied by electrons and contribute to a negative charge, thereby enhancing the dark current (Figure 3).

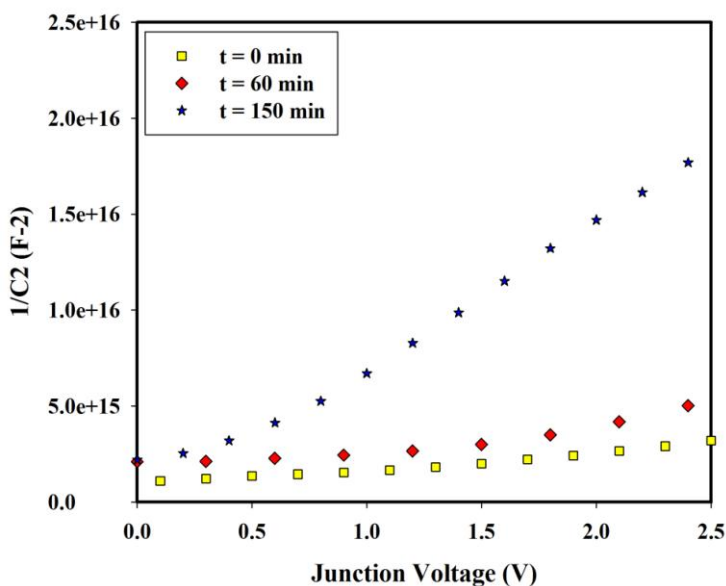


Figure 7. Gamma radiation effect on $1/C^2$ versus voltage characteristic for monocrystalline solar cell measured at 10 kHz.

This behavior was consistent with the following equation:

$$J_0 = A^*T^2 e^{-q\Phi_b/kT} \tag{19}$$

where A^* is the Richardson constant, Φ_b is the barrier height.

Figure 8 shows the scanning electron micrographs of the front and cross-section views of the Ag/Al contacts. In cross sectional view of figure 8 the upper layer represents aluminium followed by a thicker layer of Ag contacts. The layer of aluminium also helps to protect the silver contacts that are present below it.

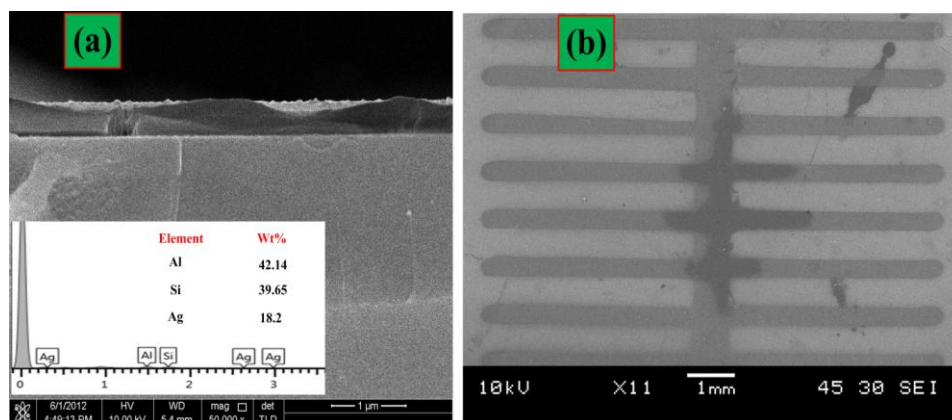


Figure 8. (a) FESEM image of cross sectional view of the solar cell contacts (b) SEM image of front view.

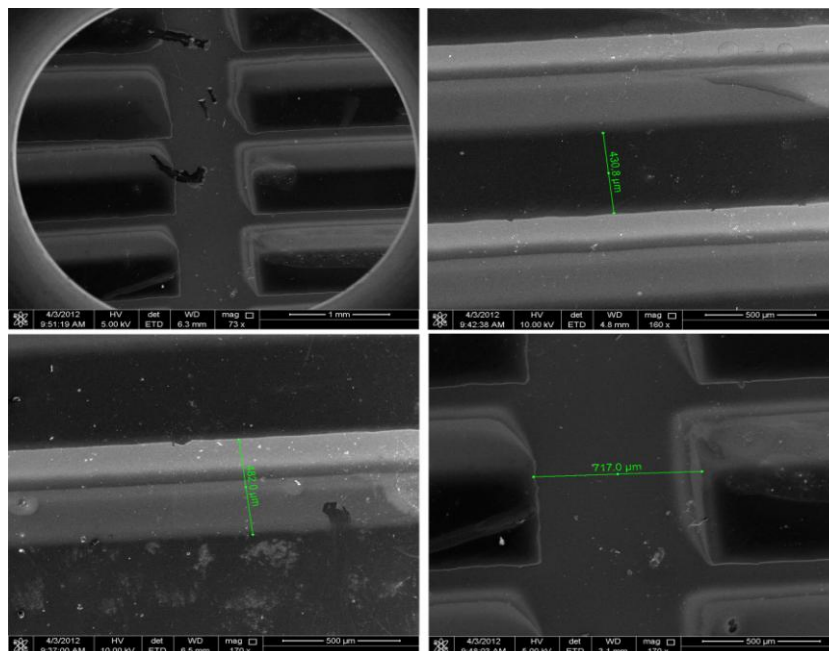


Figure 9. FESEM images of the dimensions of the contacts used in the experiment.

The combination of these two metals helps to collect more negative charge carriers from the semiconductor. The dimensions of the metal contacts used in the experiment are shown in Figure 9.

4. CONCLUSION

The experimental results confirmed that the $I-V$ and $C-V$ characteristics of the Si solar cells were strongly affected by γ -ray irradiation. I_{sc} and V_{oc} decreased, whereas dark $C-V$ characteristics increased with the increasing exposure time of monocrystalline Si solar cells to γ -radiation. High C values at low frequencies were attributed to excess C . This phenomenon was controlled by the recombination centers or energy states produced inside the band gap after γ -ray irradiation. These additional energy states affected the electrical characteristics of the monocrystalline Si solar cells, thereby reducing overall efficiency. The results indicated that the degradation of the properties might be attributed to the introduction of radiation-induced lattice defects by displacement damage.

ACKNOWLEDGEMENT

The authors acknowledged the Short Term Research Grant Scheme (1001/PFIZIK/845015), Exploratory Research Grant Scheme (203/PFIZIK/6730051) and Universiti Sains Malaysia (USM) for the Fellowship to Khuram Ali.

References

1. R. J. Walters, S. R. Messenger, H. L. Cotal, G. P. Summers and E. A. Burke, *Solid-State Electron.* 39 (1996) 797.

2. O. Tuzun, S. Altındal, S. Oktik, *Renew. Energ.* 33 (2008) 286.
3. L. Musilek, P. Fowles, *Int. J. Appl. Rad. Isotopes* 33 (1982) 1473.
4. S. Asdul-Majid, *Appl. Rad. Isotopes* 38 (1987) 1057.
5. G. P. Summers, *IEEE Trans. Nucl. Sci.* 40 (1993) 1372.
6. T. P. Ma, P. V. Dressendorfer, *Ionizing radiation effect in MOS devices and circuits*, Wiley, New York, 1989.
7. M. Yamaguchi, *Sol. Energy Mater. Sol. Cells* 68 (2001) 31.
8. D. J. Curtin, R.L. Statler, *IEEE Trans. Aerospace Electron Systems* 11 (1975) 499.
9. J. Dubow, Hydrogen and methane synthesis through radiation catalysis, US DOE Report, DOE-ER-4258-T-1, (1980) 45.
10. H.Y. Tada, J.R. Carter, B.E. Anspaugh, R.G. Downing, *Solar Cell Radiation Handbook*, 3rd Edition, National Aeronautics and Space Administration, JPL Publication, Pasadena, California, (1982) 162.
11. R. D. Evans, *The Atomic Nucleus*, McGraw-Hill, New York, ch. 25 1955.
12. K. Ali, S. A. Khan, M. Z. MatJafri, *Superlattices Microst.* 52 (2012) 782–792.
13. G. Xue, Y. Guo, T. Yu, J. Guan, X. Yu, J. Zhang, J. Liu, Z. Zou, *Int. J. Electrochem. Sci.* 7 (2012) 1496.
14. J. R. Srour, C. J. Marshal and Paul W. Marshall, *IEEE transactions on nuclear science* 50 (2003) 653.
15. F. A. Junga and G. M. Enslow, *IRE Trans. Nucl. Sci.* 6 (1959) 49.
16. J. J. Loferski and P. Rappaport, *Phys. Rev.* 3 (1958) 432.
17. F. Seitz and J. S. Koehler, *Displacement of atoms during irradiation*, Solid State Physics, Academic Press, Inc., New York, 1956.
18. C. M. Davisson and R. D. Evans, *Rev. Mod. Phys.* 24 (1952)79.
19. R. Kishore, *Solid-State Electron.* 33 (1990) 1207.
20. J. M. Rafi, F. Campabadal, H. Ohyama, K. Takakura, I. Tsunoda, M. Zabala, O. Beldarrain, M.B. González, H. García, H. Castán, A. Gómez, S. Dueñas, *Solid-State Electron.* <http://dx.doi.org/10.1016/j.sse.2012.06.011>
21. S. M. Faraz, H. Ashraf, M. I. Arshad, P. R. Hageman, M. Asghar and Q. Wahab, *Semicond. Sci. Technol.* 25 (2010) 095008-7pp.
22. K. Ali, S. A. Khan, M. Z. Mat Jafri, *Chalcogenide Lett.* 9 (2012) 457.
23. C. Sah, *Fundamentals of solid state electronics*, World Scientific Publishing, USA, 1991.
24. T. Vdovenkova, A. Vetrov, S. Kilchitskaya, T. Kilchitskaya, G. Popova, V. Strikha. *Solid-State Electron.* 38 (1995) 1929.
25. H. Neuhaus, B. Kuhlmann, R. Meyer, A. Metz, R. Auer, A. Aberle, R. Hezel, Determination of the dominant current mechanisms in the MIS tunnel diode of MIS inversion-layer silicon solar cells, 2nd World Conference and Exhibition on Photovoltaic Solar Energy Conversion, Vienna, Austria (1998) 194.
26. W. Hamdi, *J. Mater. Sci. Mater. Electron.* 8 (1997) 409.
27. H. Card, E. Rhoderick, *J. Phys. D Appl. Phys.* 4 (1971) 1589.
28. R. D. Evans, *The Atomic Nucleus*, McGraw-Hill Book Co., Inc., New York, N. Y., ch. 23, 1955.
29. D. E. Lea, *Actions of Radiations on Living Cells*, The Macmillan Company, New York, Ch. 18, Sec. 4, 1947.
30. M. M. Soliman, *Renew. Energ.* 23 (2001) 483.